ADVANCED HEALTHCARE MATERIALS
www.advhealthmat.de

Effect of Donor Age and Liver Steatosis on Potential of Decellularized Liver Matrices to be used as a Platform for iPSC-Hepatocyte Culture

*Aylin Acun, Letao Fan, Ruben Oganesyan, Korkut M. Uygun, Heidi Yeh, Martin L. Yarmush, and Basak E. Uygun**

Decellularization of discarded whole livers and their recellularization with patient-specific induced pluripotent stem cells (iPSCs) to develop a functional organ is a promising approach to increasing the donor pool. The effect of extracellular matrix (ECM) of marginal livers on iPSC-hepatocyte differentiation and function has not been shown. To test the effect of donor liver ECM age and steatosis, young and old, as well as no, low, and high steatosis livers, are decellularized. All livers are decellularized successfully. High steatosis livers have fat remaining on the ECM after decellularization. Old donor liver ECM induces lower marker expression in early differentiation stages, compared to young liver ECM, while this difference is closed at later stages and do not affect iPSC-hepatocyte function significantly. High steatosis levels of liver ECM lead to higher albumin mRNA expression and secretion while at later stages of differentiation expression of major cytochrome (CYP) 450 enzymes is highest in low steatosis liver ECM. Both primary human hepatocytes and iPSC-hepatocytes show an increase in fat metabolism marker expression with increasing steatosis levels most likely induced by excess fat remaining on the ECM. Overall, removal of excess fat from liver ECM may be needed for inducing proper hepatic function after recellularization.

1. Introduction

Orthotopic liver transplantation is a successful approach to treating end-stage liver diseases and acute liver failure,[1] however, the national and worldwide donor shortage leads to the death of patients while on the waitlist.[2] According to Organ Procurement and Transplantation Network and Scientific Registry of Transplant Recipients 2021 Annual Data Report, as of December 31, 2021, over 11 000 patients were on the waiting list for a liver transplant, in the US alone.[3] Tissue-engineered organs are an alternative to increasing the organ donor pool, which would potentially decrease the deaths due to organ scarcity. However, engineering large and highly vascular organs, such as the liver, is challenging as traditional bottom-up approaches are not suitable for developing such large-scale tissues and organs.[4] Instead, the decellularization of unused donor organs provides a natural scaffold where the composition, architecture, and vascular pathways of the organ are preserved.[5] It is reported that in 2020, 9.5% of all livers recovered were discarded,[3] which shows that there is a potential to increase the donor pool by approximately 10% since recellularization of these scaffolds with patient-specific induced pluripotent stem cell (iPSC)-derived cells may help reduce the organ shortage.

Although very promising, the use of decellularized organ scaffolds needs to be more thoroughly investigated in terms of cell-extracellular matrix (ECM) interactions. This is specifically important in utilizing organs that were deemed unusable for transplantation since such organs come with a myriad of problems. Reasons for rejection for transplant include but are not limited to; the advanced age of the donor, prolonged ischemia time, high levels of steatosis, and history of liver disease of the donor.[6] These conditions primarily affect the cells of the liver and thus are considered suitable for decellularized graft development. It has been increasingly recognized that the liver ECM changes due to different factors including age and liver diseases.[7-10] In our previous study, we investigated the differences in liver ECM due to donor age.[8] We observed that the donor age significantly affected the ECM composition and organization where older donors had livers with denser

A. Acun, L. Fan, R. Oganesyan, K. M. Uygun, M. L. Yarmush, B. E. Uygun
Center for Engineering in Medicine and Surgery
Massachusetts General Hospital
Harvard Medical School
Boston, MA 02114, USA
E-mail: basakuygun@mgh.harvard.edu
A. Acun, L. Fan, R. Oganesyan, K. M. Uygun, H. Yeh, M. L. Yarmush, B. E. Uygun
Shriners Children's
Boston, Boston, MA 02114, USA
A. Acun
Department of Biomedical Engineering
Widener University
Chester, PA 19013, USA
M. L. Yarmush
Department of Biomedical Engineering
Rutgers University
Piscataway, NJ 08854, USA

The ORCID identification number(s) for the author(s) of this article can be found under https://doi.org/10.1002/adhm.202302943

DOI: 10.1002/adhm.202302943

ECM networks and had higher collagen and glycosaminoglycan (GAG) content. In addition, the older liver ECM had a lower growth factor content compared to young liver ECM. We showed that these differences led to significant changes in primary rat and human hepatocyte metabolism as the cells cultured on old liver ECM showed lower CYP activity, and albumin and urea secretion. However, how age-related changes in liver ECM would affect the iPSC-derived cell behavior has not been explored.

In addition to age, the high-fat content of livers is another important reason for discarding donor livers. According to a study by Jackson et al. in 2017, 43.1% of the steatotic donor livers that were recovered for transplantation were discarded.[11] According to a study by Ward et al., 48.9% of adults are projected to be obese, and 24.2% of adults are projected to be severely obese by 2030 in the US.[12] Thus, it is expected that steatotic livers will more likely be used for the development of engineered livers. However, if decellularization of steatotic livers yields usable scaffolds and how the ECM of such livers will affect iPSC-derived hepatocyte function is not explored. In this study, we investigated the effect of age-related changes, as well as of steatosis on the appearance and organization of the liver ECM. Importantly, we explored the effect of such marginal livers' ECM on the development of iPSC-derived hepatocytes and their overall function when cultured in contact with these ECM scaffolds. We achieved successful decellularization of aged and young whole human livers, as well as livers with no, low, and high levels of steatosis. Using the digested ECM from these livers, we then differentiated iPSCs to hepatic lineage in their respective sandwich culture. Following differentiation, we determined the iPSC-hepatocyte function and assessed how the steatosis level of donor liver ECM affected the fat metabolism in primary human hepatocytes and iPSC-hepatocytes.

2. Results

2.1. Donor Age Leads to Changes in ECM Structure of Decellularized Human Livers

We decellularized human livers that were not suitable for transplantation using our previously established protocol.[8] We confirmed the success of decellularization through histological analysis, as well as through assessing DNA content before and after decellularization. Our results showed that regardless of donor age, the decellularization was achieved homogeneously throughout the livers. This was evident as the color of all livers changed to transparent/white at the end of decellularization (**Figure 1**A,B), and the DNA content following decellularization was less than 50 ng per mg tissue for both young and old livers (Figure S1A, Supporting Information). The homogeneity of cellular content removal can be observed through the uniform color change of the livers, as well as through the small standard deviation in DNA content analysis, since the results shown represent samples collected from eight different regions in livers. These results are further supported by the histological analysis where hemotoxylin and eosin (H&E) staining shows abundant presence of nuclei prior to decellularization ($T = 0$), and absence of cellular materials after decellularization (decellularized) (Figure 1C,D).

We also assessed the effect of donor age on ECM structure in decellularized human livers. Both H&E and trichrome staining of liver sections showed that the old livers had a denser ECM structure compared to young livers (Figure 1C,D and Figure S1B, Supporting Information). The overall collagen content assessment also supports this finding as a higher collagen content was measured for old livers compared to young livers, after decellularization (Figure S1C, Supporting Information).

2.2. Age-Related Changes in Liver ECM Led to Differences in iPSC Differentiation to Hepatocytes

To understand the effects of age-related changes in ECM on human iPSC differentiation to hepatocytes, we cultured iPSCs and induced their differentiation when cultured in a sandwich culture of young and old hDLM. Cells differentiated in Geltrex sandwich culture were used as a control since substrates, such as Geltrex or Matrigel, are the gold standard for iPSC culture, maintenance, and differentiation. We investigated the mRNA expression of markers specific to different key stages of differentiation (**Figure 2**A). The first step in differentiation is the derivation of a definitive endoderm (DE). While both young and old hDLM induced higher expression of endoderm markers GATA binding protein 4 (GATA4) and SRY-box transcription factor 17 (SOX17) compared to Geltrex controls, young hDLM induced over five times higher GATA4 mRNA expression compared to old hDLM (relative GATA4 mRNA expression: 46.4 ± 0.9-fold in young hDLM, 8.4 ± 0.8-fold in old hDLM, $p < 0.001$) (Figure 2B). A similar trend was observed in the expression of early hepatic markers cytokeratin 19 (CK19) and alpha-fetoprotein (AFP) (Figure 2C).

Specifically, CK19 expression was affected by liver hDLM presence and donor age as cells differentiated in young hDLM had 54.6 ± 0.4-fold expression while it was 12.2 ± 0.5-fold in old hDLM ($p < 0.01$). AFP expression showed similar levels for culture in Geltrex and old hDLM, while young hDLM induced a higher level of expression (relative AFP mRNA expression: 3.5-fold in young hDLM, $p < 0.01$ compared to both Geltrex and old hDLM).

Following the hepatoblast specification (HS) stage, the cells reach the hepatoblast stage and are induced to expand during the hepatoblast expansion (HE) stage. From this stage forward, we monitored the expression of mature hepatic markers to assess their increase as differentiation progressed. The expression of tyrosine aminotransferase (TAT) and AFP showed donor age-related changes as young hDLM induced significantly higher levels of expression (Figure 2D). Interestingly, CYP2B6 and albumin expression were similar in young and old hDLM. Although albumin expression levels did not change in response to culture in the liver matrix, CYP2B6 expression was induced 4.4 ± 0.7-fold in young hDLM and 5.2 ± 0.8-fold in old hDLM. We also determined the expression of AFP at this stage and observed that compared to the HS stage the expression levels remained unchanged in both young and old hDLM, relative to Geltrex.

In the immature hepatocyte derivation (IHC) stage of differentiation, expression levels of CYP3A4, CYP2B6, and TAT showed a donor age-dependent difference as their expression was significantly higher in young hDLM compared to both Geltrex and old hDLM (Figure 2E). CYP2D6 and CYP1A2 expression was also observed to be higher in young hDLM compared to old hDLM and Geltrex, although this difference was not significant. Interestingly, albumin expression showed a drastic

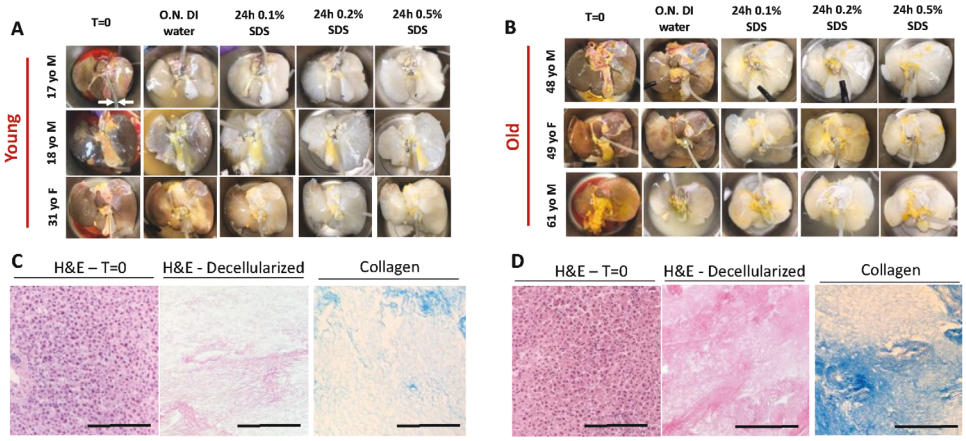

Figure 1. Donor age leads to differences in overall appearance and ECM structure of decellularized livers. The pictures of livers from A) young (aged 17–31), and B) old (aged 48–61) donors throughout the decellularization process. The H&E staining of liver sections before ($T = 0$) and after (decellularized) decellularization, as well as trichrome staining of liver sections after decellularization from C) young, and D) old donor livers (white arrows in panel (A) show the portal vein cannula with a diameter of 1 cm) (scale bars = 200 μm).

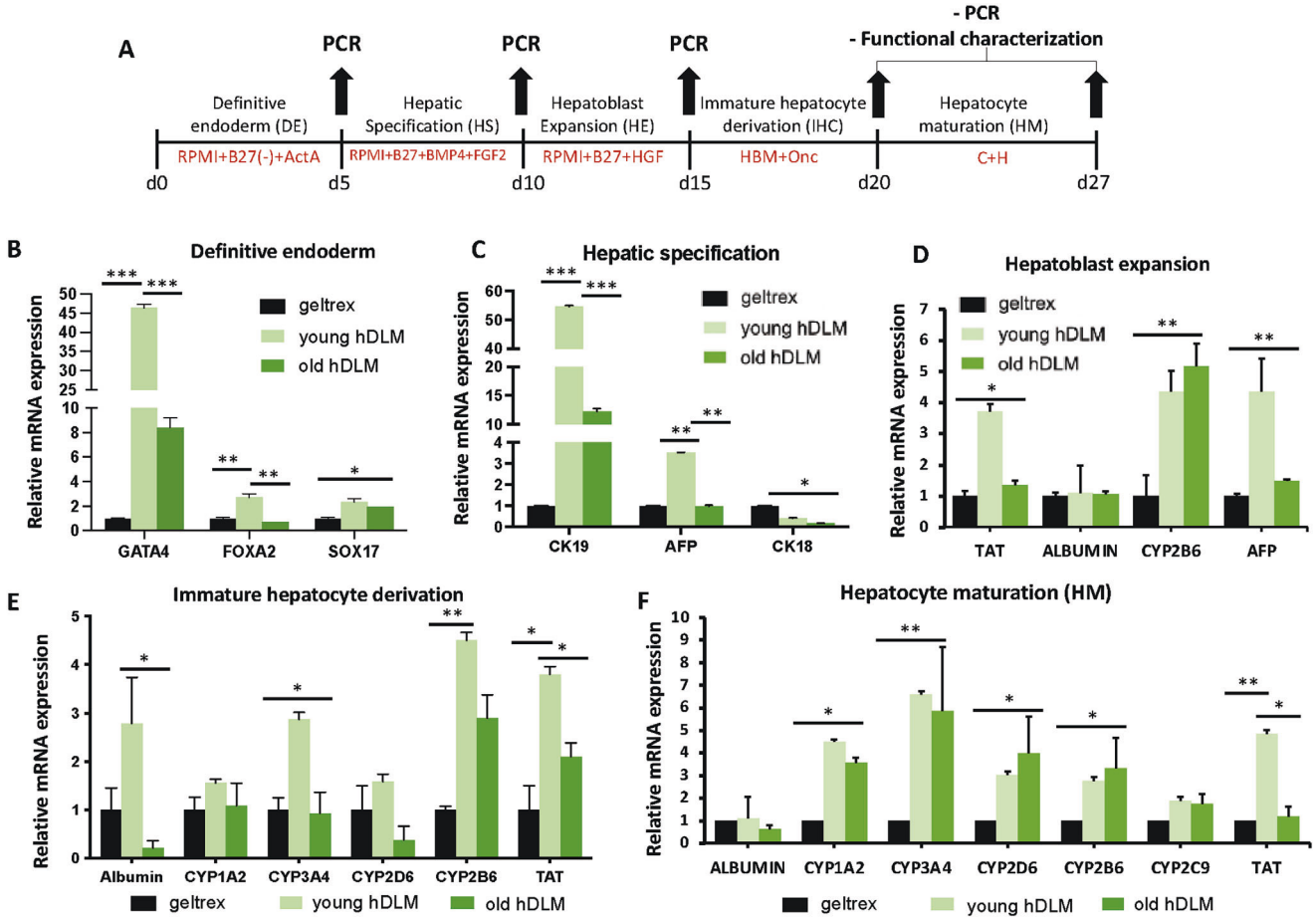

Figure 2. The mRNA expression levels of key markers specific to each differentiation stage show changes with liver donor age. A) The schematic representation of the differentiation and analysis timeline. The qRT-PCR analysis showing the mRNA expression of B) endoderm markers at the DE stage and C) early hepatic markers at the HS stage in iPSCs differentiated on young and old hDLM relative to iPSCs differentiated on Geltrex. The mRNA expression of mature hepatic markers at D) HE stage, E) IHC stage, and F) HM stage, relative to iPSCs differentiated on Geltrex (statistical significance is shown by * $p < 0.05$, ** $p < 0.01$, ***$p < 0.001$) (Student's t-test, $n = 3$).

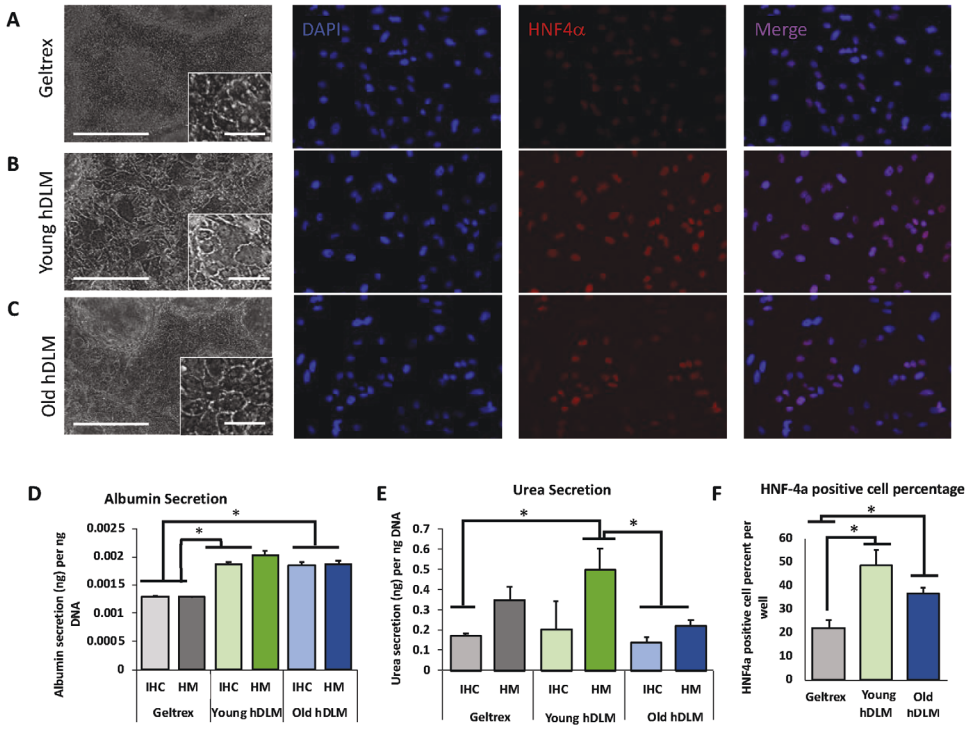

Figure 3. Donor age-related changes in hDLM leads to changes in urea secretion and HNF-4α expression. The phase/contrast and fluorescence images of iPSC-hepatocytes differentiated on A) Geltrex, B) young hDLM, and C) old hDLM. D) The albumin secretion (ng albumin/ng DNA), and E) urea secretion (ng urea/ng DNA) in iPSC-hepatocytes differentiated on Geltrex, young hDLM, and old hDLM. F) The percent HNF-4a positive cells in iPSC-hepatocytes differentiated on Geltrex, young hDLM, and old hDLM (scale bars = 400 μm, inset scale bars = 50 μm) (statistical significance is shown by * $p < 0.05$) (Student's *t*-test, $n = 3$).

change as differentiation progressed from HE to IHC stage in an age-dependent manner. The cells differentiated in young hDLM showed a significantly higher expression of albumin (2.8 ± 0.9-fold) compared to both Geltrex and old hDLM (0.2 ± 0.1-fold). Finally, as hepatocyte maturation was induced, expression of CYP1A2, CYP3A4, and CYP2D6 showed an increase in both young and old hDLM compared to the IHC stage (Figure 2F). This increase was more prominent for the old hDLM group since in the IHC stage expression of CYP2D6, CYP3A4, and CYP2B6 for the old hDLM was lower than that of the young hDLM group, however, they equalized at hepatocyte maturation (HM) stage. At this stage, the only difference in expression between cells differentiated in young versus old hDLM was observed for TAT. Consistent with HE and IHC stages, at the HM stage, TAT expression remained highest for young hDLM while it was similar for Geltrex and old hDLM. At the HM stage, we also assessed CYP2C9 expression levels and observed that although a higher expression was induced by young and old hDLM, the difference between these groups and Geltrex control was not significant.

2.3. Liver Donor Age Affects Protein Expression and Secretion in iPSC-Hepatocytes

We determined the effect of age-related changes in hDLM on hepatocyte nuclear factor 4 alpha (HNF-4α) expression and albumin and urea secretion. We did not observe significant morphological differences in the iPSC-hepatocytes when cultured on Geltrex, young hDLM, or old hDLM (**Figure** 3A–C, left). HNF-4α expression, however, showed differences relative to the culture surface (Figure 3D). The quantification of HNF-4α positive cells showed that, when cultured on Geltrex, only 21.7 ± 3.4% of cells were expressing HNF-4α. This percentage increased to 36.6 ± 2.5% when cultured on old hDLM, and to 48.5 ± 6.8% when cultured on young hDLM. Although no statistical difference was observed between young and old hDLM, both liver matrices led to a significant increase in HNF-4α expression compared to Geltrex controls (Geltrex vs young hDLM, $p = 0.019$, and Geltrex vs old hDLM, $p = 0.038$). Albumin secretion showed a similar trend where culturing on hDLM led to a significant increase in albumin secreted per ng DNA (Figure 3E). Albumin secretion was determined at the IHC and HM stages in all conditions.

Although no significant difference was observed between the two stages regardless of the culture surface, a slight increase was observed in young hDLM cultures. The secreted albumin level at the HM stage on the Geltrex surface was 0.0013 ng albumin per ng DNA, which increased to 0.0019 on old hDLM and to 0.002 on young hDLM (Geltrex vs young hDLM, $p = 0.015$, and Geltrex vs old hDLM, $p = 0.024$). The urea secretion on the other hand showed a significant difference related to the differentiation stage when cultured on young hDLM (Figure 3F). At the IHC stage of differentiation, iPSC-hepatocytes secreted 0.20 ± 0.13 ng urea per ng DNA, which increased to 0.50 ± 0.11 at the HM stage of differentiation on young hDLM ($p = 0.045$). In addition, a significant

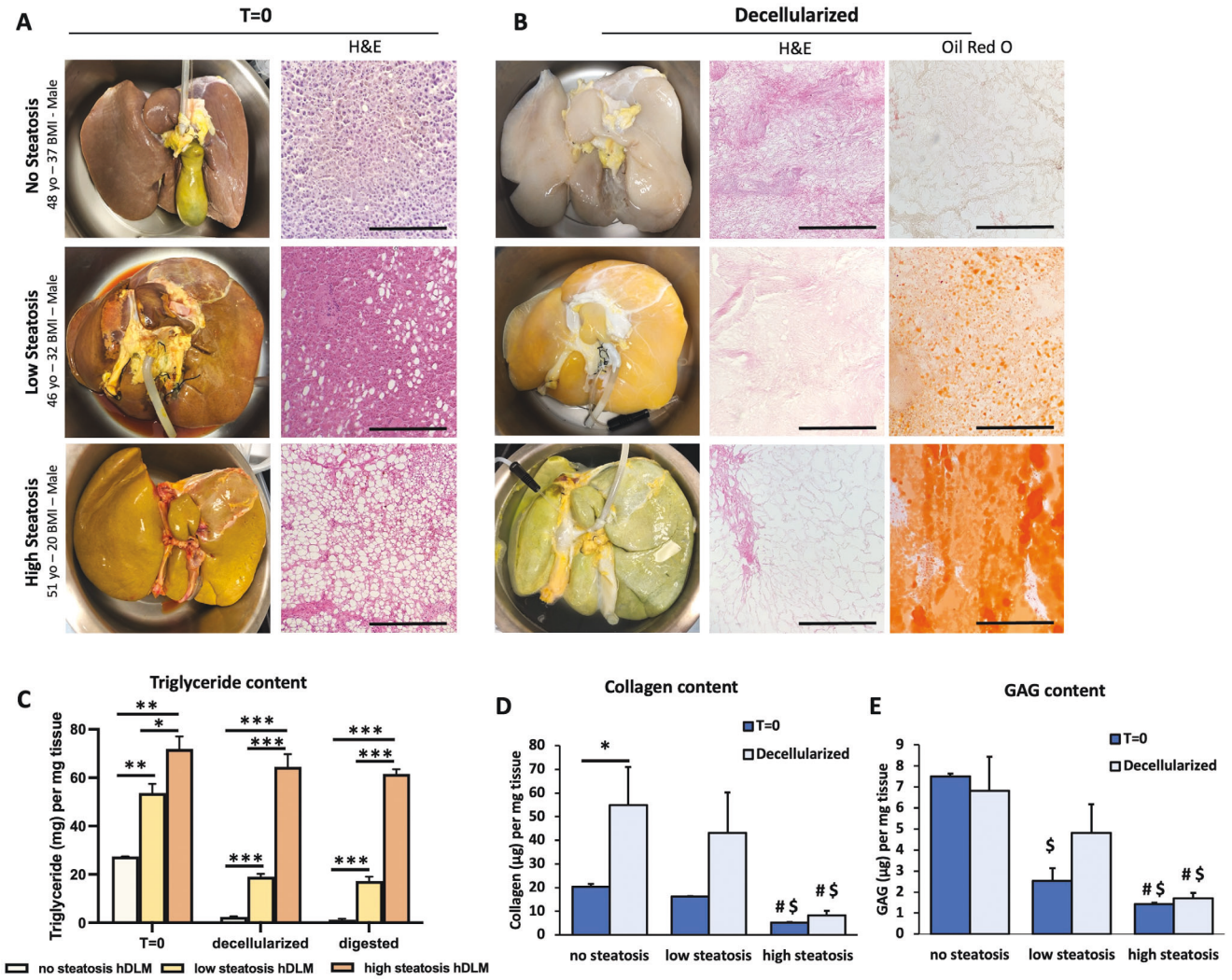

Figure 4. Different steatosis levels lead to different levels of fat remaining on hDLM. A) The pictures and H&E staining of livers with no steatosis, low steatosis, and high steatosis before decellularization. B) The pictures, H&E staining, and oil red o staining of livers with no steatosis, low steatosis, and high steatosis after decellularization. C) The triglyceride content (mg triglyceride per mg tissue) of livers before ($T = 0$) and after (decellularized) decellularization as well as after pepsin digestion (digested) and filtration (filtered). D) The collagen content, and E) the GAG content of no steatosis, low steatosis, and high ($T = 0$) and after (decellularized) decellularization (Scale bars = 200 µm) (Statistical significance is shown by * $p < 0.05$, ** $p < 0.01$, ***$p < 0.001$) ($ indicates statistical significance when compared to no steatosis hDLM, and # indicates statistical significance when compared to low steatosis hDLM) (Student's *t*-test, $n = 3$).

difference was observed between young hDLM compared to Geltrex (only at the IHC stage) and old hDLM (at both IHC and HM stages) groups. At the HM stage old hDLM group had 0.22 ± 0.03 ng urea per ng DNA secreted which was significantly lower than the young hDLM ($p = 0.014$). At the same stage, the Geltrex group had 0.35 ± 0.06 ng urea secreted per ng DNA. Although this value is lower than the young hDLM group, significance was not achieved ($p = 0.12$).

2.4. Donor Liver Steatosis Level Yields hDLMs with Different Levels of Fat Accumulation after Decellularization

To determine the effect of different levels of steatosis on hDLM quality and the related effects on iPSC-hepatocyte generation and function, we decellularized livers from three different donors with varying levels of steatosis: i) no steatosis, ii) low steatosis, and iii) high steatosis (**Figure** 4A). The steatosis level of livers was determined by observing the histological sections before decellularization, considering the fat droplets within the liver tissue qualitatively. Our protocol successfully yielded decellularized livers regardless of the steatosis level of the livers. This was evident by the color change observed through the decellularization, as well as the remaining DNA amount in all livers being lower than 50 ng DNA per mg tissue, after decellularization (Figure S1D, Supporting Information). We also assessed the histological sections from these livers following whole liver decellularization for morphology (Figure 4B, left and middle), as well as remaining fat content (Figure 4B, right). We observed through H&E staining that the liver with high steatosis showed a much less dense

ECM structure compared to the other livers. The Oil Red O staining showed that fat retention on ECM increased with the level of steatosis.

Our quantitative triglyceride (TGA) assay confirmed these results showing that both before and after decellularization TGA content significantly increased with steatosis level (Figure 4C).

At the end of the whole liver, decellularization biopsies were collected from different parts of the livers and the average TGA content was found to be 2.4 ± 0.3 mg TGA per mg tissue for no steatosis liver, 19.1 ± 1.2 for low steatosis, and 64.5 ± 5.1 for high steatosis liver (low vs high steatosis livers $p = 0.00011$, high vs no steatosis livers, $p = 3.1 \times 10^{-5}$ and low vs no steatosis, $p = 1.9 \times 10^{-5}$).

In order to develop the sandwich cultures using hDLMs, the liver ECM is digested using pepsin to prepare them into an ECM gel. We assessed if pepsin treatment would cause significant changes in the TGA content of hDLMs. Our results showed that there was no significant difference within the groups when compared after decellularization and after digestion. Since the high steatosis hDLM had an unusual coloration and fat accumulation even after digestion, we also applied syringe filtration to this group to remove the excess fat that was separated from the ECM. The filtration step did not change the TGA content of the ECM itself, only the excess fat layer which was separated from the ECM was removed (data not shown).

We also assessed if different steatosis levels in donor livers led to differences in collagen and GAG content. We observed an increase in collagen content per mg tissue following decellularization, which was significant only for no steatosis hDLM (Figure 4D). Importantly, after decellularization high steatosis hDLM had the lowest collagen content with 8.3 ± 1.8 µg collagen per mg tissue, which was significantly lower than both no steatosis hDLM ($p = 0.018$), and low steatosis hDLM ($p = 0.035$). The GAG content did not show significant changes when compared before and after decellularization within the groups (Figure 4E). However, similar to collagen content, high steatosis hDLM had the lowest GAG content with 1.7 ± 0.2 µg GAG per mg tissue after decellularization. This was significantly lower than after decellularization values for no steatosis hDLM ($p = 0.015$), and low steatosis hDLM ($p = 0.028$).

2.5. Difference in Steatosis Level in Donor Livers Leads to Different Marker Expression throughout the Differentiation of iPSCs

We used hDLMs of different steatosis-level donor livers to develop respective sandwich cultures of undifferentiated iPSCs. The cells were then differentiated and mRNA expression of markers in different differentiation stages was assessed. Geltrex was used as the control for hDLMs where all results are represented in comparison to iPSCs differentiated to the respective stage on Geltrex. At the DE stage, the highest expression levels for GATA4 and SOX17 were observed on high steatosis hDLM (GATA4: 12.2 ± 5.3-fold, SOX17: 14.9 ± 1.9-fold), which was significantly higher than all other groups (**Figure 5A**). FOXA2 mRNA expression, however, was observed to be the highest in the low steatosis hDLM group (154.9 ± 11-fold). At the HS stage, mRNA expression of early hepatic markers CK18 and CK19 were assessed (Figure 5B). Expression of both markers was significantly higher in no and low steatosis hDLMs compared to the Geltrex group. CK19 expression did not show any significant changes related to hDLM steatosis levels. CK18 expression, however, was observed to be the highest in no steatosis hDLM (3.7 ± 0.2-fold), which was significantly higher than all other groups.

To assess marker expression at later stages of differentiation, we determined mature hepatic marker mRNA expression in the IHC and HM stages. At IHC stage, a trend was observed where expression of TAT, CYP1A2, CYP2C9, CYP3A4, and CYP2D6 were the highest on low steatosis hDLM compared to all other groups (TAT: 150401 ± 1.1-fold, CYP1A2: 115.6 ± 3.3-fold, CYP2C9: 231.44 ± 50.4-fold, CYP3A4: 719.7 ± 201.5-fold, CYP2D6: 46.5 ± 3.2-fold) (Figure 5C). Only the expression of albumin was the highest on high steatosis hDLM with 1651.7 ± 569.9-fold, which was significantly higher than all other groups. Expression of TAT, CYP1A2, CYP2C9, CYP3A4, and CYP2D6 was lowest in the Geltrex group, although the difference was not significant for all markers. Following 7 days of maturation, at the HM stage, the expression pattern of the same mature hepatic markers showed changes (Figure 5D). Expression of TAT, CYP1A2, CYP2C9, and CYP2D6 significantly increased on high steatosis hDLM compared to the IHC stage. Specifically, CYP1A2 and CYP2C9 expression reached similar levels on low steatosis and high steatosis hDLMs (CYP1A2: 4.2 ± 1.4-fold in low steatosis hDLM, 4.4 ± 2.1-fold in high steatosis hDLM; CYP2C9: 8.8 ± 0.3-fold in low steatosis hDLM, 7.9 ± 1-fold in high steatosis hDLM). CYP3A4 expression also showed an increase in no, low, and high steatosis groups compared to the IHC stage (CYP3A4 at HM stage: 34.4 ± 2.7-fold in no steatosis, 5141.2 ± 13.8-fold in low steatosis, and 3477.8 ± 5.7-fold in high steatosis hDLM).

Expression of all markers was significantly lower on no steatosis hDLM, compared to other hDLM groups (due to low values of expression, bars representing no steatosis group are not well visible in Figure 5D. The expression values are as follows: TAT: 1.2 ± 0.05, CYP1A2: 0.25 ± 0.002, CYP2C9: 0.07 ± 0.006, CYP3A4: 34.4 ± 2.7, CYP2D6: 0.4 ± 0.004, and Albumin: 0.04 ± 0.03-fold). In addition, expression of CYP1A2, CYP2C9, CYP2D6, and albumin was higher in the Geltrex group compared to no steatosis hDLM. Expression of albumin remained significantly higher than all other groups on high steatosis hDLM at 59.7 ± 6.2-fold. In addition to differences in marker expression on different substrates, we quantitatively observed more and larger fat droplets in high-fat hDLM samples (Figure 5E).

In addition to mRNA expression, we also assessed the albumin and urea secretion of differentiated hepatocytes on IHC and HM stages (**Figure 6A,B**). At the HM stage, consistent with mRNA expression, the highest urea secretion was recorded on high steatosis hDLM (Figure 6A) with 322.1 µg albumin per well. Although there was no difference between IHC and HM stages on low fat hDLM, we observed an increase in albumin secretion as the cells matured on Geltrex and no steatosis hDLM groups. This increase (from 101.4 ± 11.1 at IHC to 236.1 ± 53.8 µg albumin per well at HM stage) was significant on no steatosis hDLM ($p = 0.02$) and not significant on Geltrex ($p = 0.41$). Similar to albumin secretion, urea secretion was the highest at the HM stage on high steatosis hDLM with 22.7 ± 10.7 ng urea per well (Figure 6B). Although a slight increase was observed, no groups showed a significant increase in urea secretion going from the IHC to the

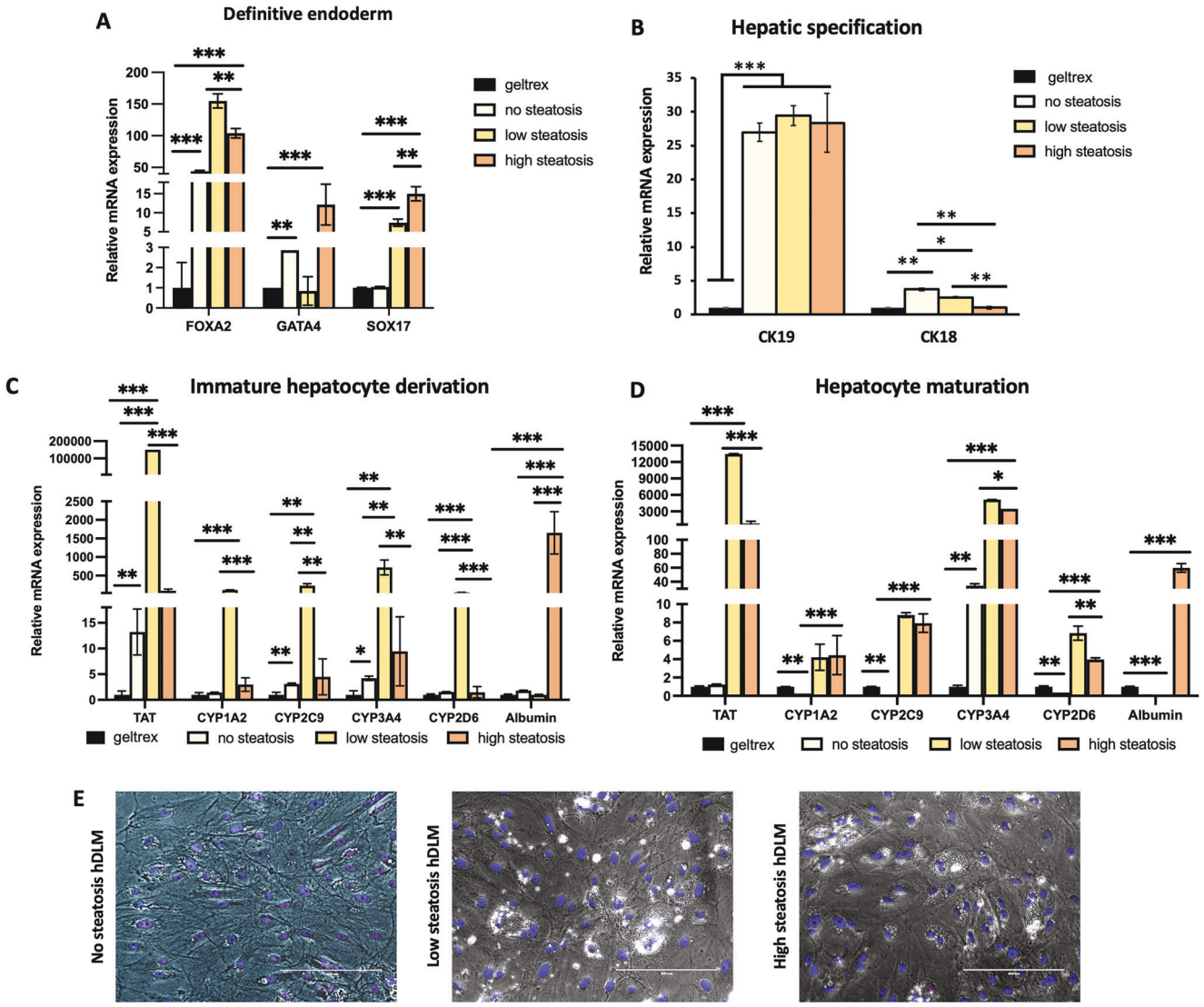

Figure 5. The mRNA expression levels of key markers specific to each differentiation stage show change with the steatosis level of donor livers. The qRT-PCR analysis showing the mRNA expression of A) endoderm markers at the DE stage. B) The mRNA expression of early hepatic markers at the HS stage. The mRNA expression of mature hepatic markers at C) IHC stage, and D) HM stage, relative to undifferentiated iPSCs. E) The phase/contrast images with nuclear stain (blue) of iPSC-hepatocytes at HM stage, differentiated on no, low, or high steatosis hDLM (Scale bars = 400 μm) (Statistical significance is shown by * $p < 0.05$, ** $p < 0.01$, ***$p < 0.001$) (Student's t-test, $n = 3$).

HM stage. The only significance was recorded between no steatosis IHC versus high steatosis HM ($p = 0.039$) and between low steatosis IHC versus high steatosis HM ($p = 0.043$).

2.6. Donor Liver Steatosis Affects Fat Metabolism in iPSC-Hepatocytes and Primary Human Hepatocytes

In addition to differentiation, we assessed if the iPSC-hepatocyte and primary hepatocyte interaction with the steatotic liver microenvironment would affect the fat metabolism of the cells. We first quantified the cellular TGA content in iPSC-hepatocytes at the IHC and HM stages (Figure 6C). These two stages were compared to determine the effect of the maturation step on cell fat metabolism. For all hDLM substrates there was a slight increase in cellular TGA content going from IHC to HM stage, although this change was non-significant ($p = 0.056$ for no steatosis, $p = 0.060$ for low steatosis, and $p = 0.101$ for high steatosis). At the IHC stage, the high steatosis hDLM group showed significantly higher TGA levels (75.9 ± 1.4 ng TGA per ng RNA) compared to Geltrex controls (59.8 ± 3.7 ng TGA per ng RNA, $p = 0.044$) and low steatosis hDLM (59.3 ± 3.1 ng TGA per ng RNA, $p = 0.023$).

The mRNA expression of several fat metabolism markers, namely, acetyl-CoA carboxylase alpha (ACACA), acyl-CoA synthetase long-chain family member 4 (ACSL4), fatty acid synthase (FASN), and fatty acid binding protein 5 (FABP5) were also investigated in response to culture on hDLMs at HM level (Figure 6D,E). Expression of all markers was significantly higher when iPSC-hepatocytes were cultured on high steatosis hDLM (Figure 6D). The most significant increase in mRNA expression

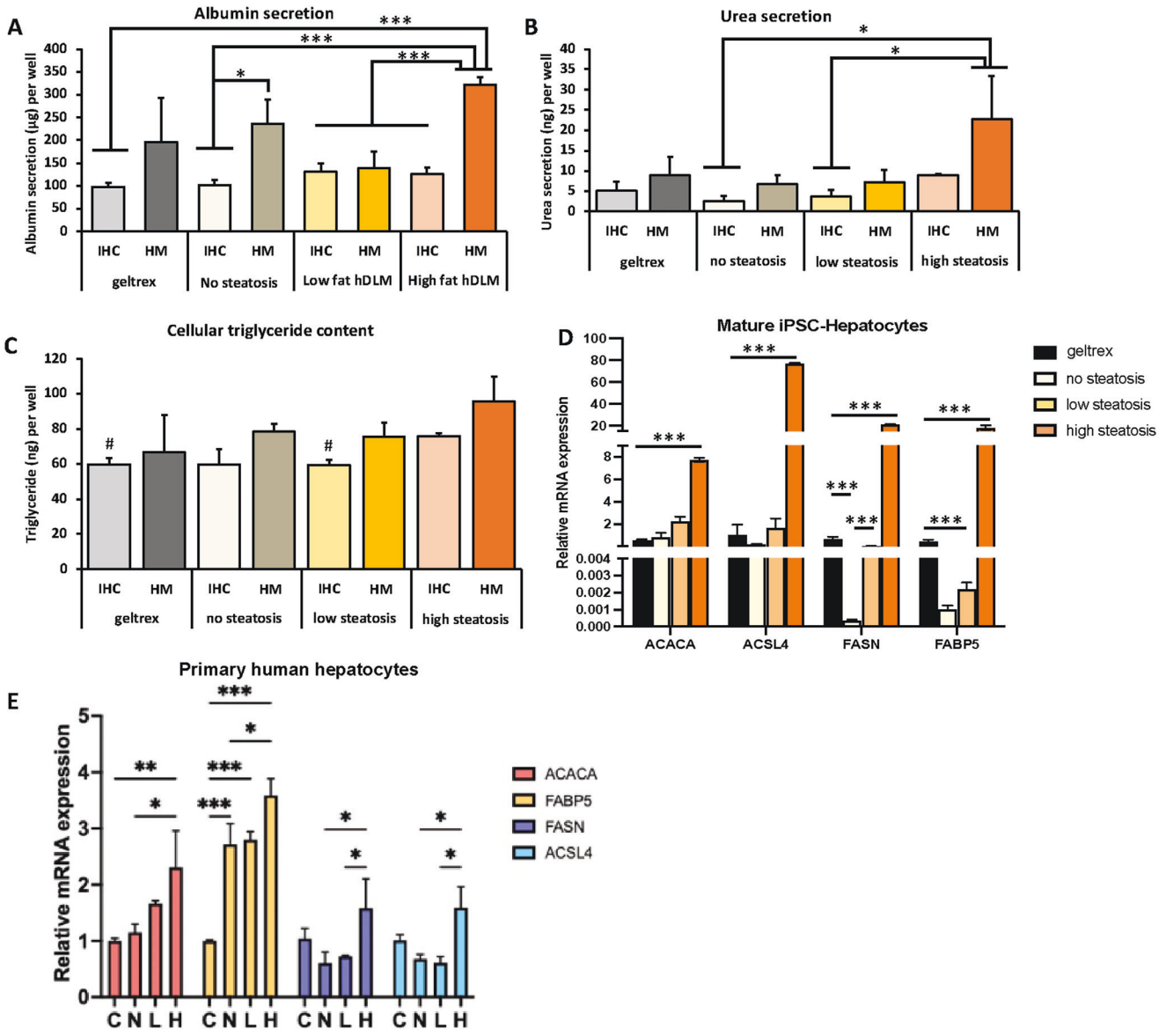

Figure 6. iPSC-hepatocytes and primary human hepatocytes show increase in fat metabolism enzyme mRNA expression upon exposure to high steatosis hDLM. Quantification of A) albumin secretion, B) urea secretion, C) cellular triglyceride content of iPSC-hepatocytes at IHC and HM stages when differentiated on Geltrex, no steatosis, low steatosis, and high steatosis hDLM. The qRT-PCR analysis showing the mRNA expression of fat metabolism markers ACACA, ACSL4, FASN, and FABP5 in (D). iPSC-hepatocytes at HM stage, and E) in primary human hepatocytes when cultured on no steatosis, low steatosis, and high steatosis hDLM relative to Geltrex and collagen, respectively (Statistical significance is shown by * $p < 0.05$, ** $p < 0.01$, ***$p <$ 0.001) (# represents significant difference ($p < 0.05$) compared to high fat hDLM at IHC stage) (Student's *t*-test, $n = 3$).

was recorded for ACSL4. In high steatosis, hDLM ACSL4 expression was 77.2 ± 0.3-fold, whereas it was 1.7 ± 0.8-fold for low steatosis and 0.21 ± 0.04-fold for no steatosis hDLMs. Although a slight yet not significant increase in expression was recorded for ACACA, ACSL4, and FABP5 in low steatosis hDLM compared to no steatosis hDLM, there was a significant increase in expression of FASN when the same two groups are compared (FASN expression: 0.034 ± 0.010-fold in low steatosis hDLM, and 0.00040 ± 0.00004-fold in no steatosis hDLM).

In order to compare our findings with primary hepatocytes, we cultured human hepatocytes in a sandwich culture of collagen (as control), no steatosis, low steatosis, and high steatosis hDLM for 4 days and assessed the mRNA expression of fat metabolism markers (Figure 6E). We observed a trend similar to iPSC-hepatocytes where high steatosis hDLM had significantly higher expression of ACACA and FABP5 than collagen and no steatosis hDLM. Fold expression of ACACA in high fat hDLM was 2.27 ± 0.5 as compared to 1.15 ± 0.3-fold in no steatosis and 1.67 ± 0.1 in low steatosis hDLM ($p = 0.0014$ for high vs no steatosis hDLM, $p = 0.15$ for high vs low steatosis hDLM). The highest expression levels were observed for FABP5 expression in high steatosis hDLM with 3.6 ± 0.5-fold, compared to 2.8 ± 0.3-fold in

low steatosis and 2.7 ± 0.7-fold in no steatosis hDLM ($p = 0.03$ for high vs no steatosis hDLM, $p = 0.06$ for high vs low steatosis hDLM).

In addition, high steatosis hDLM had significantly higher expression compared to no and low steatosis hDLM groups for FASN and ACSL4 (FASN: $p = 0.013$ for high vs no steatosis, $p = 0.035$ for high vs low steatosis hDLM; ACSL4: $p = 0.023$ for high vs no steatosis, $p = 0.013$ for low vs high steatosis hDLM). Overall the fold difference between high steatosis hDLM and other groups was not as large as observed in iPSC-hepatocytes. In addition, similar to what we observed with Geltrex controls, collagen controls showed similar expression levels for markers ACACA, ACSL4, and FASN. FABP5 expression of all hDLM groups was significantly higher than collagen controls.

3. Discussion

The population in the U.S. is progressively getting older. According to the Population Reference Bureau, by 2050, one-fifth of the total population is projected to be aged 65 or older.[13] In addition, the 2021 National Health Statistics Reports state that the obesity prevalence between 2017 and 2020 was 41.9%[14] which is projected to increase to almost half the U.S. population by the year 2030.[12] These projections indicate that more and more marginal livers may be available for organ engineering in efforts to increase the donor pool. Thus, it is crucial to understand if the scaffolds developed using such marginal livers have any adverse effects on cell function.

Here, we used our previously developed whole liver decellularization protocol[8] to develop liver scaffolds from aged and steatotic livers. Our results showed that the protocol did not require any alterations to accommodate the age or steatosis level of the livers. Both aged livers and low and high steatosis livers were successfully decellularized as all livers had less than 50 ng DNA per mg tissue, which is the standard to establish sufficient decellularization,[15] along with the absence of nuclear content in H&E staining.[16] Histological analysis of the livers showed, consistent with our earlier findings, that aged livers had a denser ECM structure and higher collagen content compared to young livers. We observed the opposite pattern with increasing steatosis levels. The liver with high steatosis had a less dense ECM morphology compared to non-steatotic and low steatosis livers. Histological analysis of this liver showed disturbed morphology potentially caused by the well-known characteristic of steatosis, enlargement of hepatocytes through excessive lipid accumulation,[17] leading to the formation of large pores after decellularization. The higher collagen and GAG content in livers with no steatosis also supports the less dense ECM structure in the high steatosis liver.

Importantly, in addition to the structural ECM characteristics, we investigated the effectiveness of iPSC differentiation to hepatic lineage and induced hepatocyte function when cultured with the aged and steatotic liver ECMs. Cell-ECM interactions are known to be responsible for taking part in regulating cell growth, differentiation, and migration.[18] The age-related changes in ECM composition and structure have been shown to affect the cell function in various tissues including skin,[19] skeletal muscle,[20] heart,[21] and liver.[8,22] In our previous study, we showed that the native liver ECM gels made from decellularized livers of 18-month-old rats and of 46–52-year-old human donor livers lead to deterioration in rat and human primary hepatocyte function.[8] Here we investigated how iPSC differentiation to hepatocytes is affected by donor age-related changes in the liver ECM. iPSCs and induced hepatocytes are abundantly available and can provide patient-specific cells for organ engineering, and thus are a promising cell source for future applications. It was shown that iPSC differentiation to hepatocytes is most successful when the cells are placed in contact with the liver ECM at the earliest stages of differentiation.[23] Thus, we started and maintained the differentiation of iPSCs to hepatocytes in sandwich cultures of young and old hDLMs. At early stages of differentiation (DE and HS stages), endoderm and early hepatic marker expression were significantly lower in old hDLM cultures. Brafman and colleagues showed that fibronectin and vitronectin promoted DE differentiation in human embryonic stem cells (ESCs).[24] Our previous study showed that old hDLM had higher fibronectin content. However, we also showed that the old rat liver matrix had significantly lower levels of bFGF.[8] Another study showed that DE differentiation of human ESCs was induced when cells were exposed to bFGF, Activin A, and BMP4.[25] Therefore, our results potentially suggest that the higher bFGF content in young hDLM, when combined with external supplementation of Activin A (at DE stage) and BMP4 (at HS stage) may be overcoming the lower levels of fibronectin, leading to higher levels of endoderm and early hepatic marker mRNA expression.

When we explored the marker expression in later stages of differentiation, we observed that the young hDLM did not induce significantly higher expression levels on all markers. Specifically, at HM stage, expression of albumin, CYP3A4, CYP2D6, CYP2B6, and CYP2C9 were expressed at similar levels on young and old hDLM. This could be at least partially due to the increased collagen type I, laminin, and fibronectin presence in old hDLM compared to young hDLM.[8] Flaim and colleagues investigated the effect of different combinations of 5 liver ECM proteins on the differentiation of mouse ESCs to hepatocytes.[26] Their results showed the combination of collagen type I, laminin, and fibronectin led to the highest expression of cellular albumin and that of fetal liver-specific gene *Ankrd17*. This synergistic effect between these ECM proteins and differentiation could explain how old hDLM and young hDLM yielded similar expression of albumin and CYPs. This is also supported by our observation of secreted albumin amount and HNF-4a positive cell percent not having a statistically significant difference between young and old hDLM. Although albumin secretion did not show any difference, urea secretion at the HM stage was higher in young hDLM compared to old hDLM. This is consistent with previously observed primary human hepatocyte urea secretion on old hDLM.[8]

Due to the increasing prevalence of obesity and morbid obesity in the U.S., it is crucial to explore the potential of steatotic livers for use in liver engineering. Following confirmation of successful decellularization of the low and high steatotic livers and the non-steatotic liver, we explored the TGA and lipid content remaining on the decellularized ECM. TGA content analysis showed that the fat content of no steatosis liver was mostly cellular and was almost completely removed through decellularization. The low and high steatosis livers, however, had a significant level of fat remaining on the ECM as shown by TGA levels and Oil Red O staining. Our results are the first to show the decellularization of steatotic livers

to the best of our knowledge. However, the decellularization of other tissues with high-fat content, such as adipose tissue, has been shown.[27–29] Usually, following the decellularization of adipose tissue, an additional step of defatting is carried out using lipase or isopropanol treatment. In our study, we aimed to investigate the effect of ECM in its form immediately after decellularization without additional defatting steps.[30] Thus, we digested the liver ECM, which did not alter the TGA content of ECM significantly, and then used the resulting hDLMs as a substrate for iPSC differentiation. We observed two of the DE markers investigated to be expressed significantly higher in high steatosis hDLM compared to no and low steatosis hDLM. Hosseini et al. reported that using a small molecule inhibitor of stearoyl-coenzyme A desaturase 1 (SCD1), which is needed for the synthesis of fatty acids, leads to the maintenance of pluripotent state in iPSCs as opposed to endoderm differentiation.[31] They also showed that oleate exposure along with SCD1 inhibitor rescued the endodermal differentiation. Along with this report, the well-known role of fatty acids in regulating iPSC differentiation[32] can potentially explain the increase in endodermal marker expression in high steatosis hDLM since this matrix contains the highest fat content. At the HS stage of differentiation, we did not observe the same pattern. Early hepatic marker CK19 expression showed no difference with respect to steatosis levels, while expression of CK18 showed a decrease with increasing steatosis. Varghese and colleagues performed a global transcriptome analysis on iPSCs derived from normal and genetically obese patients through different stages of differentiation to hepatocytes.[33] The cells were tested with or without palmitic acid treatment. Authors noted that at hepatoblast derivation stage of differentiating normal iPSCs with or without palmitic acid treatment showed no significant difference in early hepatic marker expression, suggesting that the external factors are less significant in later stages of differentiation.

At the IHC stage of differentiation, low steatosis hDLM yielded the highest expression of CYP450 enzymes investigated. Interestingly the albumin expression was significantly higher both in IHC and HM stages in the high steatosis hDLM group compared to all others. Albumin and urea secretion analysis showed the highest rates in the high steatosis hDLM group at the HM stage, consistent with the high albumin mRNA expression, while at the IHC stage, we did not observe the same correlation. A primary hepatocyte-based 3D perfused in vitro model of NAFLD showed that the cells exposed to high fat conditions had impaired CYP3A4 and CYP2C9 activity, while albumin production was significantly increased.[34] Donato and colleagues also showed a decline in both mRNA expression, and activity of CYP1A2, CYP2A6, CYP2B6, CYP2C9, CYP3A4, CYP2D6, and CYP2E1in primary human hepatocyte model of steatosis created by exposing cells to 1 mM free fatty acid mixture.[35] Similarly, the expression of TAT was shown to be downregulated in high-fat high sugar diet treated NAFLD mice models.[36] Thus, the lower expression of CYP450 enzymes and TAT could be caused by the high-fat content in high steatosis hDLM. Interestingly, we observed that mRNA expression of CYP450 enzymes showed an increase at the HM stage compared to the IHC stage in no and high steatosis hDLMs. Expression of CYP1A2 and CYP2C9 reached similar levels as the low steatosis hDLM group as expression decreased in low steatosis, and increased in no and high steatosis groups. Although expression of CYP2D6 and CYP3A4 was still significantly higher in low steatosis hDLM, the gap between high and low steatosis groups was reduced considerably. Similarly, the gap in expression levels of TAT between low and high steatosis groups was also reduced at the HM stage. One potential explanation for this change could be the consumption of excess fat deposited on high steatosis hDLM. Since the HM stage is achieved in 7 days, this period could have led to a decrease in the overall fat content of the high steatosis hDLM by the cells. We also observe no significant difference in cellular TGA levels at the HM stage between different groups, while at the IHC stage, cellular TGA is significantly higher than the low steatosis hDLM group. Further studies exploring the TGA levels in hDLM following cell culture are necessary to support this hypothesis.

We also observed a significant difference in expression levels of mature hepatic markers between no steatosis and low steatosis hDLM groups: mRNA expression of all markers explored was lower in no steatosis hDLM. This could be driven by the fat content of low steatosis hDLM increasing fat consumption and hepatocyte metabolism while not inducing the adverse effects of high-fat exposure. Lyall et al. investigated the CYP3A4 activity in human ESC-derived hepatocyte-like cells treated with lactate, pyruvate, and octanoic acid at low and high doses, compared to untreated controls.[37] Although not significant, CYP3A4 activity in untreated cells was lower than the low-dose treatment. In this study, we used a single liver for each condition due to the availability of donor livers thus, we do not take into account the donor–donor variability under different steatosis levels. Future studies with a higher number of samples for each group are needed to confirm the results and strengthen the conclusions drawn regarding their comparison.

Finally, we assessed the mRNA expression of fat metabolism markers at the HM stage in both iPSC-hepatocytes and primary human hepatocytes. We observed an increase in the expression of ACACA, FASN, ACSL4, and FABP5 with hDLM steatosis level. The difference in expression between high steatosis hDLM compared to no and low steatosis groups was more prominent in iPSC-hepatocytes. ACACA and FASN are responsible for fatty acid synthesis, and ACSL4 also plays a key role in lipid biosynthesis and fatty acid degradation. FABP5 plays a role in the uptake, transport, and metabolism of fatty acids. Overall, the increased expression of these markers is potentially due to the higher fat content of the hDLM derived from high steatosis donor liver. Upregulation of ACACA and FASN was also shown in human ESC-derived hepatocytes that were fed a high fat-containing media, which was noted to resemble the NAFLD profile.[37] Aljabban and colleagues assessed the transcriptome changes in NAFLD liver sections. Compared to normal (<5% steatosis) livers, they noted upregulation in FABP5 along with other genes involved in lipogenesis.[38] Other studies[39,40] have also shown a strong correlation between fat accumulation in the liver and the upregulation of FABP5, ACSL4, and ACACA. The observation of a similar increase in these factors in primary human hepatocytes suggests that excess fat remaining on ECM collected from highly steatotic livers may lead to a NAFLD-like phenotype in liver cells.

4. Conclusion

In conclusion, we show here that marginal donor livers due to advanced age or high steatosis can be successfully decellularized.

The ECM extracted from these livers allows for the differentiation of iPSCs into hepatocytes. After maturation, the old age of donor livers does not yield different mRNA expressions of hepatic markers. However, a significantly lower urea secretion and non-significantly lower HNF-4a expression suggest that the age-related changes in liver ECM may be causing functional deterioration in iPSC-hepatocytes. In addition, for the first time to our knowledge, we show whole human liver decellularization of livers with different steatosis levels, and the effect of these scaffolds on iPSC differentiation, hepatocyte function, and fat metabolism. Although high steatosis in the donor liver leads to lower expression of mature hepatic markers at the IHC stage, following the maturation step this difference diminishes. High steatosis donor livers lead to significantly higher urea and albumin secretion, however, potentially the excess fat accumulated on the ECM also leads to upregulation of lipogenesis and other fat metabolism markers to be overexpressed, resembling an expression pattern observed in NAFLD patients. Taken together, steatotic livers can be decellularized using established techniques, however, an additional step of defatting using lipase or isopropanol treatment can be added to limit the adverse effects of excess fat remaining in the scaffold. Future studies where more donor livers of similar steatosis levels are tested with and without excess fat removal will provide crucial insight into the potential use of such marginal livers in organ engineering. Although steatosis does not play a role in the fetal development of liver, in liver engineering applications it has been shown that the iPSC interaction with native liver matrix has been shown to induce differentiation to mature hepatocyte-like cells, thus can be preferred as a recellularization strategy. This renders the study of the effect of liver ECM steatosis on iPSC differentiation of importance. Despite being out of the scope of this study, the determination of the specific mechanisms that trigger better hepatic maturation in steatotic decellularized livers should be studied in more detail to shed light on the molecular contributors of this phenomenon. In addition, livers deemed old in this study range between age 48 and 61, and future work investigating the effects of donor liver age over 65 will be valuable in understanding the increasingly growing supply of older donor livers available for organ engineering.

5. Experimental Section

Human Liver Decellularization: Donor human livers unsuitable for transplantation were provided by New England Donor Services. This study was declared exempt by the MGB IRB (2011P001496). A total of nine human livers were decellularized. Six of these livers were grouped according to age as young ($n = 3$; 17-year-old, 18-year-old, and 31-year-old) and old ($n = 3$; 48-year-old, 49-year-old, and 61-year-old). Three livers with similar donor ages were categorized according to their steatosis levels as no steatosis ($n = 1$, 48-year-old), low steatosis ($n = 1$, 46-year-old), and high steatosis ($n = 1$, 51-year-old) depending on the histological analysis prior to decellularization. None of the donors were listed to have a history of liver disease and detailed demographics are provided in Table S1, Supporting Information. The livers were maintained frozen at −80 °C until decellularization. To start decellularization, the livers were cannulated at the portal vein and hepatic artery. Livers were perfused at different flow rates at the two cannulas (80 mL min^{-1} from the portal vein and 40 mL min^{-1} from the hepatic artery). The flow rate was increased periodically (5 min every hour for 12 h each day) to 180 mL min^{-1} for the portal vein and to 90 mL min^{-1} for the hepatic artery to flush out cell debris. In addition, the livers were massaged to physically induce the removal of cell debris for 5 min every hour for 12 h each day of decellularization.

The decellularization of whole human livers was achieved following the previously developed protocol.[8] Briefly, livers were sequentially perfused with deionized (DI) water (16 h), 0.1% sodium dodecyl sulfate (SDS) (Sigma Aldrich) (24 h), 0.2% SDS (24 h), and 0.5% SDS (24 h). The livers were then washed with DI water for 2 h, 1% Triton X-100 (Millipore Sigma) for 2 h, and finally with PBS for 3 h. For DNA, collagen and GAG quantification biopsy samples were collected from each liver right before starting decellularization ($T = 0$) at the tip of the left lobe and the end of decellularization from the right lobe tip, right lobe center, left lobe tip, left lobe center, caudate lobe center, and quadrate lobe center.

Development of Decellularized Human Liver Matrices for Cell Culture: To develop the representative young and old human liver matrices for cell culture, discarded young (19-year-old male ($n = 1$)), old (60-year-old female ($n = 1$)), no steatosis (48-year-old male ($n = 1$)), low steatosis (46-year-old male ($n = 1$)), and high steatosis (51-year-old male ($n = 1$)) donor human livers were used (provided by New England Donor Services). None of the donors were listed as having a history of liver disease (Table S1, Supporting Information). The liver matrix microenvironment for cell culture was envisioned as a matrix gel to mimic the primary hepatocyte sandwich culture. To develop liver matrix gels, sections of the human livers (4 × 4 × 4 cm) were dissected and frozen at −20 °C for at least 1 h, and 50-µm thick slices were cryosectioned. Following the previously established protocol,[8] decellularization was achieved by incubating the liver sections subsequently in DI water (16 h), 0.01% SDS (3 h), and 0.1% SDS (1.5 h) with agitation. This was followed by 1% Triton X-100 (1.5 h) and at least five times PBS washes (30 min each) to remove excess SDS and Triton X-100 from the matrices. The resulting matrices, or hDLM were lyophilized and stored at 4 °C until further use.

All hDLM were digested using pepsin for solubilization to be used as a cell culture substrate.[23] Briefly, the hDLM was incubated in 1 mg mL^{-1} pepsin (Sigma Aldrich) solution (at pH = 2) for 24 h at room temperature (RT) to give a concentration of 10 mg hDLM per 1 mL pepsin solution, with constant agitation. The final concentration of the solubilized hDLM was assessed by removing undigested ECM and determining its weight following freeze drying. The solubilized hDLM was then diluted to 1.25 mg mL^{-1} final concentration using 0.01 M HCl. All solubilized hDLM were stored at 4 °C until use.

Histological Analysis: The liver samples collected before ($T = 0$) and after decellularization (decellularized) were fixed with formalin (10% v/v) for 24–48 h at RT followed by incubation in 70% ethanol at 4 °C. The tissues were then dehydrated through incubation in higher concentration ethanol stepwise and embedded in paraffin. To visualize the ECM and cell nuclei, the tissues were micro-sectioned into 5-µm thick slices and stained with hematoxylin (Leica) and eosin (Leica) (H&E). In addition, collagen fibers in decellularized liver tissues were assessed using Masson's Trichrome staining of 5-µm thick slices using standard protocols. The stained sections were imaged using the Nikon Eclipse E800.

Oil Red O staining was performed by first air drying the sections for 30 min. The sections were then fixed using formalin (10% v/v) and then dipped in 60% isopropanol. The slides were then stained with Oil Red O solution (2% w/v) for 15 min. Then the slides were subsequently dipped in 60% isopropanol (one time) and DI water (at least ten times) to wash off excess dye. The stained sections were imaged using the Nikon Eclipse E800.

Assessment of DNA, Total Collagen, and Sulfated Glycosaminoglycan Content: The amount of DNA in the liver samples collected before ($T = 0$) and after decellularization (decellularized) was assessed to ensure complete decellularization. DNA was isolated using a Purelink genomic DNA kit (Invitrogen) following the manufacturer's instructions. NanoDrop 1000 spectrophotometer (Thermo Fisher Scientific) was used to quantify the amount of DNA as defined by absorbance at 260-nm wavelength. The amount of DNA is represented as a weight-normalized value for all samples. The weight corrections were done against the wet weight of the tissues. DNA content for decellularized whole human livers is calculated by taking the average of the values obtained from the samples collected from

eight different locations to better represent the homogeneity throughout the liver.

The total collagen content of the liver samples collected before ($T = 0$) and after decellularization (decellularized) was assessed using a total collagen kit (QuickZyme Biosciences) following the manufacturer's instructions. The total collagen amount was calculated as µg collagen per mg tissue through normalization to tissue weights. In order to determine the total sulfated GAG content, a previously established protocol was used.[23] Briefly, the liver samples were hydrolyzed in HCl (6 M) at 95 °C for 20 h. Then, the hydrolyzed samples were mixed with 50 µM of dimethylene blue solution. The total amount of sulfated GAGs was determined by measuring absorbance at 525 nm and comparing it to dilutions of chondroitin sulfate A as standard.

Cell Culture: Human iPSC line hIPS-K3 cells, derived from skin fibroblasts, were kindly provided by Dr. Stephen Duncan (Medical College of Wisconsin). The iPSCs were maintained in Geltrex (LDEV-Free Reduced Growth Factor Basement Membrane Matrix, Gibco) coated culture flasks in mTeSR plus culture medium (Stemcell Technologies) with daily media changes until they reached 70% confluency. Throughout the culture, the pluripotency of the cells was examined by daily observation of the colony phenotype. At this point, the cells were collected using ReLeSR (Stemcell Technologies) and seeded on different hDLMs in 24 well plates for differentiation with 5 µM ROCK inhibitor supplemented mTeSR plus medium.

Cryopreserved primary human hepatocytes isolated from a 10-year-old female donor with no liver disease history, were purchased from Lonza (lot# 4227) and were maintained in sandwich culture of collagen (isolated from rat tail, 1.25 mg mL^{-1}), no steatosis, low steatosis, and high steatosis hDLM (1.25 mg mL^{-1}). Briefly, the well plates were coated with a layer of Geltrex (1:100 in cold DMEM) or hDLM for 1 h at 37 °C. The primary human hepatocytes were then seeded on the coated wells at a concentration of 2.5×10^5 cells per well. The cells were allowed to attach for 60 min and then were gently washed to remove unattached cells. The cells were then maintained for 24 h after which a top layer of collagen or hDLM was placed to finalize the sandwich culture. The cells were maintained in hepatocyte growth media (C+H) (DMEM supplemented with 10% fetal bovine serum, 0.5 U mL^{-1} insulin, 7 ng mL^{-1} glucagon, 20 ng mL^{-1} epidermal growth factor, 7.5 µg mL^{-1} hydrocortisone, 200 U mL^{-1} penicillin/streptomycin, and 50 µg mL^{-1} gentamycin).

Differentiation of iPSCs to Hepatocytes on hDLM: The well plates were coated with undiluted Geltrex or young, old, no steatosis, low steatosis, and high steatosis hDLM neutralized with 10× DMEM for 1 h at 37 °C. Geltrex-coated wells were used as control. For each group, at least five wells were seeded with iPSCs for differentiation. After coating was complete, iPSCs were seeded at a concentration of 5×10^5 cells per well and were allowed to attach for 24 h. After 24 h, the iPSCs were covered with a top layer of Geltrex or the respective hDLM. Until the start of differentiation, the iPSCs were maintained in mTeSR plus medium.

The differentiation of iPSCs to hepatic lineage was performed using a previously established protocol.[41] Briefly, the iPSCs were cultured with RPMI (1640, Invitrogen) media supplemented with 50 ng mL^{-1} Activin A (ActA) (Peprotech) and B27 without insulin (B27(-)) (Invitrogen), 10 ng mL^{-1} bone morphogenic protein 4 (BMP4) (Peprotech), and 20 ng mL^{-1} fibroblast growth factor 2 (FGF-2) (Peprotech) for 2 days. This was followed by culture for 3 days in the same media without BMP4 and FGF-2. At the end of the first 5 days of differentiation, a definitive endoderm (DE) stage was achieved. The next 5 days of differentiation involved culture of cells with RPMI containing B27 with insulin (B27(+)) (Invitrogen), supplemented with 20 ng mL^{-1} BMP4 (Peprotech) and 10 ng mL^{-1} FGF-2 (Peprotech) to achieve hepatic specification (HS) stage. Then, the cells were incubated for 5 days with RPMI containing B27 with insulin supplemented with 20 ng mL^{-1} hepatocyte growth factor (HGF) (Peprotech) to achieve the hepatoblast expansion (HE) stage. The cells were then incubated for 5 days with Hepatocyte Basal Media (HBM) (Lonza) supplemented with SingleQuots (without EGF) supplemented with 20 ng mL^{-1} Oncostatin-M (Onc) (R&D Systems) to achieve immature hepatocyte derivation (IHC) stage. Finally, the cells were cultured with C+H media for 7 days to achieve the hepatocyte maturation (HM) stage. At the end of the HM stage, the cells are referred to as iPSC-hepatocytes.

Quantitative Real-Time PCR: In order to determine mRNA expression levels of specific markers at each stage of differentiation of iPSCs, as well as that of fat metabolism markers in iPSC-hepatocytes and primary human hepatocytes, RNA was extracted from cells ($n > 5$ per stage) using PureLink RNA isolation kit (Thermofisher Scientific) following manufacturer's instructions. The resulting RNA was tested for purity and concentration using a NanoDrop 1000 spectrophotometer (ThermoFisher Scientific) and was used for cDNA synthesis using an iScript cDNA synthesis kit (Bio-Rad) following the manufacturer's instructions. The cDNA was then used in quantitative real-time PCR (qRT-PCR) analysis using the ViiA7 Real-time PCR system (Thermo Fisher Scientific) using a power SYBR Green PCR master mix kit (Thermo Fisher Scientific) according to the manufacturer's instructions. The list of primers used is provided in Table S2, Supporting Information. All expression levels were normalized to GAPDH expression. Results were represented relative to iPSCs differentiated on Geltrex-coated well plates at different stages of differentiation. Expression levels for primary human hepatocytes cultured on hDLMs were represented relative to expression in cells cultured on collagen.

Quantification of Secreted Albumin and Urea: For albumin and urea quantification, culture media was collected at the end of IHC and HM stages differentiated on Geltrex or different hDLMs. The level of secreted albumin was determined using the Human Albumin ELISA kit (Abcam), and the level of secreted urea was determined the urea nitrogen direct kit (Stanbio), following the manufacturer's instructions. The results were normalized to DNA amount per well to account for cell number differences among different samples and represented as ng albumin or urea per ng DNA.

Immunocytochemistry: The iPSC-hepatocytes differentiated on Geltrex, young, and old hDLM were immunostained for HNF-4a to show the abundance of commitment to hepatic lineage at the end of differentiation. Briefly, the cells were fixed using 4% paraformaldehyde (v/v) for 10 min at RT. Following washes with PBS, the cells were permeabilized using 0.2% Triton X-100 (v/v) for 15 min at RT. The cells were then blocked using 10% goat serum for 1 h at RT. Following blocking, the cells were incubated with mouse anti-human HNF-4a primary antibody (ThermoFisher Scientific, MA1-199) overnight at 4 °C. This was followed by PBS washes. Next, the cells were incubated with goat anti-mouse Alexa Fluor 594 (ThermoFisher Scientific) for 4 h at 4 °C. The cells were then extensively washed and stained with DAPI to visualize the nuclei. The cells were imaged using an EVOS fluorescence microscope (Thermo Fisher Scientific). For quantification, ten images were taken per well and the number of cells with and without HNF-4a expression were counted using ImageJ software. The results were represented as HNF-4a positive cell percentage per well. The standard deviation was calculated as the deviation among different wells for each group. For each group, at least five wells were used for quantification.

Quantification of Intracellular and Secreted Triglyceride Content: The TGA content of no steatosis, low steatosis, and high steatosis livers before and after decellularization, as well as that of iPSCs differentiated to IHC and HM stages on the corresponding hDLMs, was determined using Serum Triglyceride Quantification Kit (Cell Biolabs, Inc., STA-396) following manufacturer's instructions. The TGA content for tissue samples was normalized against tissue weight. The TGA content for cells was normalized per cell number per well. At least three wells per group for each stage of differentiation were used for assessment and the results are represented as average ± standard deviation.

Statistical Analysis: For all statistical analysis, Microsoft Excel Office 365 (Version 16.69.1) and GraphPad Prism (Version 9.2) were used. Student's *t*-test with Welch's correction and two-way ANOVA with Tukey's multiple comparisons test were used. Statistical difference was defined as $p < 0.05$. All results are represented as the average ± standard deviation of three different differentiation experiments using the same cell line but different cultures within passages 21–27.

Supporting Information

Supporting Information is available from the Wiley Online Library or from the author.

Acknowledgements

This study was supported by the National Institutes of Health (grant number: R01DK084053 M.L.Y. and B.E.U., grant numbers: R01DK114506 and R01DK096075 K.U.) and Shriners Children's (grant number: 84702 A.A.). This work was partially supported by the National Science Foundation (grant number: EEC 1941543 B.E.U.) and the National Institutes of Health/The National Institute of Arthritis and Musculoskeletal and Skin Diseases (grant number: R01AR082825 B.E.U.). The authors would like to acknowledge the support from Shriners Special Shared Facilities Translational Regenerative Medicine (84051), Morphology and Imaging (84050), and Genomucs and Proteomics (84090) in conducting the studies.

Conflict of Interest

The authors declare no conflict of interest.

Data Availability Statement

The data that support the findings of this study are available from the corresponding author upon reasonable request.

Keywords

aging, decellularization, iPSC-hepatocytes, liver engineering, steatosis

Received: September 3, 2023
Revised: November 13, 2023
Published online: February 21, 2024

[1] P. C. Müller, G. Kabacam, E. Vibert, G. Germani, H. Petrowsky, *Int. J. Surg.* **2020**, *82*, 22.
[2] C. B. Hughes, A. Humar, *Abdom. Radiol.* **2021**, *46*, 2.
[3] Organ Procurement and Transplantation Network (OPTN) and Scientific Registry of Transplant Recipients (SRTR). OPTN/SRTR 2021 Annual Data Report (accessed: August 2023).
[4] B. Zhang, M. Radisic, *J. Thorac. Cardiovasc. Surg.* **2020**, *159*, 2003.
[5] S. F. Badylak, D. Taylor, K. Uygun, *Annu. Rev. Biomed. Eng.* **2011**, *13*, 27.
[6] H. Mergental, R. W. Laing, A. J. Kirkham, M. T. P. R. Perera, Y. L. Boteon, J. Attard, D. Barton, S. Curbishley, M. Wilkhu, D. A. H. Neil, S. G. Hübscher, P. Muiesan, J. R. Isaac, K. J. Roberts, M. Abradelo, A. Schlegel, J. Ferguson, H. Cilliers, J. Bion, D. H. Adams, C. Morris, P. J. Friend, C. Yap, S. C. Afford, D. F. Mirza, *Nat. Commun.* **2020**, *11*, 2939.
[7] E. Arriazu, M. Ruiz de Galarreta, F. J. Cubero, M. Varela-Rey, M. P. Pérez de Obanos, T. M. Leung, A. Lopategi, A. Benedicto, I. Abraham-Enachescu, N. Nieto, *Antioxid. Redox Signaling.* **2014**, *21*, 1078.
[8] A. Acun, R. Oganesyan, K. Uygun, H. Yeh, M. L. Yarmush, B. E. Uygun, *Biomaterials.* **2021**, *270*, 120689.
[9] A. Daneshgar, O. Klein, G. Nebrich, M. Weinhart, P. Tang, A. Arnold, I. Ullah, J. Pohl, S. Moosburner, N. Raschzok, B. Strücker, M. Bahra, J. Pratschke, I. M. Sauer, K. H. Hillebrandt, *Biomaterials.* **2020**, *257*, 120247.
[10] P. Bedossa, V. Paradis, *J. Pathol.* **2003**, *200*, 504.
[11] K. R. Jackson, J. D. Motter, C. E. Haugen, C. Holscher, J. J. Long, A. B. Massie, B. Philosophe, A. M. Cameron, J. Garonzik-Wang, D. L. Segev, *Am. J. Transplant.* **2020**, *20*, 855.
[12] Z. J. Ward, S. N. Bleich, A. L. Cradock, J. L. Barrett, C. M. Giles, C. Flax, M. W. Long, S. L. Gortmaker, *N. Engl. J. Med.* **2019**, *381*, 2440.
[13] L. A. Jacobsen, M. Kent, M. Lee, *Popul. Bull.* **2011**, *66*, 2.
[14] S. Bryan, J. Afful, M. Carroll, C. Te-Ching, D. Orlando, S. Fink, C. Fryar, *NHSR 158. National Health and Nutrition Examination Survey 2017–March 2020, Pre-pandemic Data Files*, National Center for Health Statistics, U.S, **2021**.
[15] E. M. Srokowski, K. A. Woodhouse, in, *Comprehensive Biomaterials II*, (Ed.: P. Ducheyne), Elsevier, New York **2017**, p. 452.
[16] M. L. Dias, B. A. Paranhos, R. C. dos S Goldenberg, *J. Tissue Eng.* **2022**, *13*, 204173142211053.
[17] E. K. Mitten, G. Baffy, *Metab. Target Organ Damage.* **2023**, *3*, 2.
[18] C. Frantz, K. M. Stewart, V. M. Weaver, *J. Cell Sci.* **2010**, *123*, 4195.
[19] M. A. Cole, T. Quan, J. J. Voorhees, G. J. Fisher, *J. Cell Commun. Signal.* **2018**, *12*, 35.
[20] K. M. Stearns-Reider, A. D'Amore, K. Beezhold, B. Rothrauff, L. Cavalli, W. R. Wagner, D. A. Vorp, A. Tsamis, S. Shinde, C. Zhang, A. Barchowsky, T. A. Rando, R. S. Tuan, F. Ambrosio, *Aging Cell.* **2017**, *16*, 518.
[21] C. Spadaccio, A. Rainer, P. Mozetic, M. Trombetta, R. A. Dion, R. Barbato, F. Nappi, M. Chello, *J. Geriatr. Cardiol.* **2015**, *12*, 76.
[22] B. Delire, V. Lebrun, C. Selvais, P. Henriet, A. Bertrand, Y. Horsmans, I. A. Leclercq, *Aging.* **2016**, *9*, 98.
[23] M. Jaramillo, H. Yeh, M. L. Yarmush, B. E. Uygun, *J. Tissue Eng. Regener. Med.* **2018**, *12*, e1962.
[24] D. A. Brafman, C. Phung, N. Kumar, K. Willert, *Cell Death Differ.* **2013**, *20*, 369.
[25] X. Xu, V. L. Browning, J. S. Odorico, *Mech. Dev.* **2011**, *128*, 412.
[26] C. J. Flaim, S. Chien, S. N. Bhatia, *Nat. Methods.* **2005**, *2*, 119.
[27] P. M. Martin, A. Shridhar, C. Yu, C. Brown, L. E. Flynn, in *Adipose-Derived Stem Cells: Methods and Protocols*, (Eds.: B. A. Bunnell, J. M. Gimble), Springer, New York **2018**, p. 53.
[28] O. A. Mohiuddin, B. Campbell, J. N. Poche, C. Thomas-Porch, D. A. Hayes, B. A. Bunnell, J. M. Gimble, in *Cell Biology and Translational Medicine, Vol. 6: Stem Cells: Their Heterogeneity, Niche and Regenerative Potential*, (Ed.: K. Turksen), Springer International Publishing, New York **2020**, p. 57.
[29] X. Jiang, X.-R. Lai, J.-Q. Lu, L.-Z. Tang, J.-R. Zhang, H.-W. Liu, *Biochem. Biophys. Res. Commun.* **2021**, *541*, 63.
[30] S. Y. Chun, J. O. Lim, E. H. Lee, M.-H. Han, Y.-S. Ha, J. N. Lee, B. S. Kim, M. J. Park, M. Yeo, B. Jung, T. G. Kwon, *Tissue Eng. Regen. Med.* **2019**, *16*, 385.
[31] V. Hosseini, A. Kalantary-Charvadeh, M. Hajikarami, P. Fayyazpour, R. Rahbarghazi, M. Totonchi, M. Darabi, *Stem Cell Res. Ther.* **2021**, *12*, 550.
[32] L. Diamante, G. Martello, *Curr. Opin. Genet. Dev.* **2022**, *75*, 101923.
[33] D. S. Varghese, T. T. Alawathugoda, M. A. Sheikh, A. K. Challagandla, B. S. Emerald, S. A. Ansari, *Cell Death Dis.* **2022**, *13*, 670.
[34] T. Kostrzewski, T. Cornforth, S. A. Snow, L. Ouro-Gnao, C. Rowe, E. M. Large, D. J. Hughes, *World J. Gastroenterol.* **2017**, *23*, 204.
[35] M. T. Donato, A. Lahoz, N. Jiménez, G. Pérez, A. Serralta, J. Mir, J. V. Castell, M. J. Gómez-Lechón, *Drug Metab. Dispos.* **2006**, *34*, 1556.
[36] L. Xiang, Y. Jiao, Y. Qian, Y. Li, F. Mao, Y. Lu, *Genes Dis.* **2021**, *9*, 201.
[37] M. J. Lyall, J. Cartier, J. P. Thomson, K. Cameron, J. Meseguer-Ripolles, E. O'Duibhir, D. Szkolnicka, B. L. Villarin, Y. Wang, G. R. Blanco, W. B. Dunn, R. R. Meehan, D. C. Hay, A. J. Drake, , *Philos Trans R. Soc., B.* **2018**, *373*, 20170362.
[38] J. Aljabban, M. Rohr, S. Syed, K. Khorfan, V. Borkowski, H. Aljabban, M. Segal, M. Mukhtar, M. Mohammed, M. Panahiazar, D. Hadley, R. Spengler, E. Spengler, *World J. Hepatol.* **2022**, *14*, 1382.

[39] D. Greco, A. Kotronen, J. Westerbacka, O. Puig, P. Arkkila, T. Kiviluoto, S. Laitinen, M. Kolak, R. M. Fisher, A. Hamsten, P. Auvinen, H. Yki-Järvinen, *Am. J. Physiol.: Gastrointest. Liver Physiol.* **2008**, *294*, G1281.

[40] J. Westerbacka, M. Kolak, T. Kiviluoto, P. Arkkila, J. Sirén, A. Hamsten, R. M. Fisher, H. Yki-Järvinen, *Diabetes.* **2007**, *56*, 2759.

[41] K. Si-Tayeb, F. K. Noto, M. Nagaoka, J. Li, M. A. Battle, C. Duris, P. E. North, S. Dalton, S. A. Duncan, *Hepatology.* **2010**, *51*, 297.